# Dynamic Modeling and Integral Sliding Mode Controller Design for Cuk Converter under Load Variation

ByeongCheol Han[1], Minsung Kim[1], Sungho Lee[2], and Jin S. Lee[1]
[1] Department of Creative IT Engineering, POSTECH, Republic of Korea.
[2] Department of Electrical Engineering, POSTECH, Republic of Korea.

***Abstract*—A integral sliding mode controller (ISMC) for a fixed-frequency PWM is proposed for the Cuk converter. The fourth-order model of the Cuk converter is derived first and it is simplified to use ISMC. Based on the simplified system model, the ISMC that consists of the equivalent control part plus the switching control part is designed and applied to the Cuk converter in the presence of uncertain variations and unknown disturbances. The closed-loop system is also proved to be exponentially stable. Simulation and experimental tests using the prototype of digitally controlled DC-DC converter were performed to validate the proposed control approach.**

***Index Terms*—Buck-boost converter, sliding mode control, DC-DC converter, Cuk converter.**

## I. Introduction

Cuk converters are mainly applied to the dc power supplies capable of operating in step-up and step-down mode. It uses the capacitor for energy transfer, while other converters such as buck and boost converters use the inductor to do it [1]. Moreover, the Cuk converter has continuous voltage and current at both input and output terminals, thereby keeping the number of components and the component size small [5]. Cuk converters are widely used in industries such as wind energy [2], photovoltaic power system [3],[5], electrical vehicle [4] and fuel cell charger [6].

Among the controllers used for converters, proportional-integral-derivative (PID) control technique is most popular due to its simplicity and robustness. However, designing a stable Cuk converter by using the PID controller is not easy. To guarantee stable operation with the PID controller, we must use large size capacitors to decouple input and output stages. They also need to support the full-load current, and so it becomes more expensive [5]. Furthermore, PID controller often fails to perform under large parameter and load variations [7].

To utilize a low-priced and small capacitors in the Cuk converter design and attain a good performance under parameter and load variations, a number of researchers have applied SMC to Cuk converters. One of the most popular SMC is the Hysteresis-Modulation (HM)-based SMC [11], which was designed based on a complex fourth-order model [8]. And it was developed under both complete state feedback and reduced state feedback settings [9]. In practice, the Cuk converter with HM based SMC was mainly used in solar inverter, and it used much smaller, more reliable nonelectrolytic capacitors [5]. Recently, the combined PI and SMC was proposed to regulate a fourth-order Cuk converter, and its PI gains are obtained by using the Routh-Hurwitz stability criterion and root locus [10].

However, the HM-based SMC generally suffers from significant switching-frequency variation when the input voltage and the output load are varied [11, 19, 20]. This variation complicates design of the input and output filters, because oversized filters may be required to cover a worst case frequency condition. The switching frequency variation also deteriorates regulation properties of the converters. Thus, it is necessary to design SMC for the Cuk converter that operates at a constant switching frequency even under input and output variations.

SMC that operates at constant switching frequency can be developed by employing pulse width modulation (PWM) instead of HM [12]. In practice, this is similar to classical PWM control schemes in which the control signal is compared to the ramp waveform to generate a discrete gate pulse signal. The advantages of this approach is that the additional circuits are not required since the switching function is performed by the PWM modulator, and so its transient response is not deteriorated. However, PWM based SMC can cause steady-state errors [21]. Moreover, the robustness property of the conventional SMC with respect to system parameter variations and external disturbances can only be achieved in the sliding mode phase. During the reaching phase, we cannot guarantee robustness [17].

The integral sliding mode controller (ISMC) was first introduced in [13]. ISMC aims at eliminating the reaching phase so that the system robustness is guaranteed from the initial stage. PWM based ISMC was developed for Buck converter in [23] and Boost converter in [21]. In these research works, the SMC based on PWM method consists of the equivalent controller only

This research was supported by the MSIP(Ministry of Science, ICT and Future Planning), Korea, under the "IT Consilience Creative Program" (NIPA-2014-H0201-14-1001) supervised by the NIPA(National IT Industry Promotion Agency).

without any switching control function. So we propose the PWM based ISMC with a switching controller in the Cuk converter. It uses both the equivalent controller and the switching controller which enable to employ a certain sliding surface as a reference path. Simple model of the Cuk converter is derived to use the ISMC, which relatively reduces the computation burden. We prove the exponential stability of the developed Cuk converter control system. We also perform numerical simulations to test the proposed ISMC in the presence of load variation. Finally, we conducted experimental tests to demonstrate its practical feasibility.

This paper is organized as follows. In Section II, the model of the Cuk converter is derived. In Section III, dynamic equation for the Cuk converter is simplified and control design is presented. The simulation and experiment results are shown in Section IV and Section V. Finally, the conclusion is drawn in Section VI.

## II. DC-DC Cuk Converter Modeling

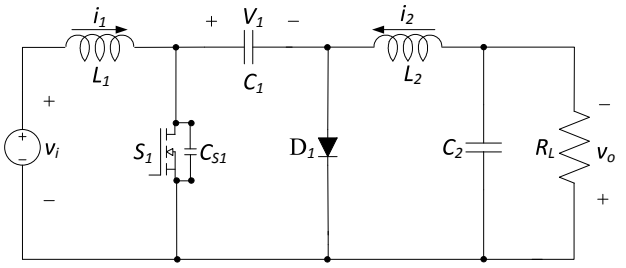


Fig. 1. The circuit diagram of Cuk Converter.

This section presents modeling of the DC-DC Cuk converter. The Cuk converter is constructed by combining a Boost converter and a Buck converter, and contains two inductor $L_1$, $L_2$, two capacitors $C_1$, $C_2$, and load resistance $R_L$ (Fig. 1). The operation principle of Cuk converter can be described as follows. When the switch $S_1$ is closed, the current flowing through the inductor $L_1$ increases. Diode $D_1$ is counterpolarized, and the capacitor $C_1$ supplies the energy to the output stage. The current that flows through the inductor $L_2$ also increases while the voltage across the capacitor $C_1$ decreases. When the switch $S_1$ is open, both inductor currents that flow through the free-wheeling diode $D_1$ decrease, and capacitor $C_1$ set recharged with current $i_1$.

The state-space equations in the turn-on and turn-off subintervals are expressed in the following equations, respectively:

$$L_1\frac{di_1(t)}{dt} = v_i(t), \tag{1}$$

$$L_2\frac{di_2(t)}{dt} = v_1(t) - v_o(t), \tag{2}$$

$$C_1\frac{dv_1(t)}{dt} = -i_2(t), \tag{3}$$

$$C_2\frac{dv_o(t)}{dt} = i_2(t) - \frac{v_o(t)}{R_L}, \tag{4}$$

and

$$L_1\frac{di_1(t)}{dt} = v_i(t) - v_1(t), \tag{5}$$

$$L_2\frac{di_2(t)}{dt} = -v_o(t), \tag{6}$$

$$C_1\frac{dv_1(t)}{dt} = i_1(t), \tag{7}$$

$$C_2\frac{dv_o(t)}{dt} = i_2(t) - \frac{v_o(t)}{R_L}. \tag{8}$$

where $i_1(t)$ is the current that flows through the input inductor $L_1$, $i_2(t)$ is the current that flows through the output inductor $L_2$, $v_1(t)$ is the voltage across the transfer capacitor $C_1$, and $v_o(t)$ is voltage across the output capacitor $C_2$. $v_i(t)$ and $v_o(t)$ respectively represent the input and output voltages, and $R_L$ represents the resistive load.

Combining (1)–(4) and (5)–(8) using the state-space averaging method, the averaged model equations can be described as

$$\frac{di_1(t)}{dt} = \frac{1}{L_1}v_i(t) - \frac{1}{L_1}(1-D)v_1(t), \tag{9}$$

$$\frac{di_2(t)}{dt} = \frac{1}{L_2}Dv_1(t) - \frac{1}{L_2}v_o(t), \tag{10}$$

$$\frac{dv_1(t)}{dt} = -\frac{1}{C_1}Di_2(t) + \frac{1}{C_1}(1-D)i_1(t), \tag{11}$$

$$\frac{dv_o(t)}{dt} = \frac{1}{C_2}i_2(t) - \frac{1}{R_LC_2}v_o(t), \tag{12}$$

where $D$ is the control duty ratio.

## III. Control scheme

### A. Simplified dynamic equation for output voltage control

The above dynamic equations (9)–(12) can be used to construct the sliding mode controllers. But the direct use of the above dynamic equations for controller design is too complex, because the four-dimension matrix needs to be solved, and the four parameters need to be measured. Instead, we suggest to use the following simplified dynamic equations for output voltage control of the Cuk converter. Taking the time derivative on both sides of (12) and substituting both (10) and (12) into the this derivative equation, we have

$$\frac{dx_1(t)}{dt} = x_2(t), \tag{13}$$

$$\frac{dx_2(t)}{dt} = f(x_1(t), z_1(t)) + g(z_2(t))u(t) + v(t), \tag{14}$$

$$y_1(t) = x_1(t), \tag{15}$$

where $\mathbf{x}(t) = [x_1(t), x_2(t)] = [v_o(t), \frac{1}{C_2}i_2(t) - \frac{1}{R_LC_2}v_o(t)]$, $z_1(t) = i_2(t)$, $z_2(t) = v_1(t)$ are the state, $y_1(t)$ is the output, $u(t) = D$ is the control input, $f(x_1(t), z_1(t))$ and $g(z_2(t))$ are the system function and the control gain, and $v(t)$ is a lumped uncertainty;

$f(x_1(t), z_1(t))$ and $g(z_2(t))$ are represented as

$$f(x_1(t), z_1(t)) = \left(-\frac{1}{L_2C_2} + \frac{1}{(R_LC_2)^2}\right) x_1(t) - \frac{1}{R_LC_2^2} z_1(t), \quad (16)$$

$$g(z_2(t)) = \frac{1}{L_2C_2} z_2(t), \quad (17)$$

and

$$v(t) = \Delta v(x_1(t), z_1(t), z_2(t), d(t)) \quad (18)$$

where $d(t)$ is the unknown external disturbance. This uncertainty satisfies the matching condition

$$v(t) \in \text{span}(g(z_2(t))). \quad (19)$$

The objective of the controller is to drive the output voltage of the Cuk converter to follow a reference output voltage in the presence of uncertain parameters and unknown disturbances. The lumped uncertainty $v(t)$ may deteriorate the control performance and even cause the system to go unstable. To overcome the problem, we propose an integral sliding mode controller (ISMC) for the Cuk converter in the following section. The aim of the ISMC is to constrain the output voltage of the Cuk converter to stay on a sliding surface $s(t) = 0$, and thereby keeping the error variables stay on the prescribed error dynamics.

### *B. Integral sliding mode controller design for the Cuk converter*

To help better understand the integral sliding mode controller, we start with choosing the sliding manifold of the conventional sliding mode controller, which is well known for its robustness to parameter uncertainties and external disturbances [18]. The conventional sliding surface is defined as $s(t)$ where

$$s(t) = \left(\lambda + \frac{d}{dt}\right)^{n-1} e_1(t), \quad (20)$$

where $n$ denotes the system order, $e_1(t) = y_{1d}(t) - y_1(t)$ represents the tracking error, $\lambda$ is a positive constant; $y_{1d}(t)$ is the reference output voltage.

In addition to the robustness property against the parameter uncertainties and disturbances, the ISMC improves the steady-state accuracy by including the integral action to the conventional sliding surface. The integral augmented sliding surface is given as [13]:

$$s(t) = (\lambda + \frac{d}{dt})^{n-1} e_1(t) + k_i \int_0^t e_1(\tau) d\tau - \left(\lambda + \frac{d}{dt}\right)^{n-1} e_1(0), \quad (21)$$

where $k_i$ is a positive constant.

We now set the system order $n = 2$ and take the derivative of the integral augmented sliding surface $s(t)$ with respect to time:

$$\dot{s}(t) = \ddot{e}_1(t) + \lambda \dot{e}_1(t) + k_i e_1(t). \quad (22)$$

Substituting (13) and (14) into (22) yields

$$\dot{s}(t) = \ddot{y}_{1d}(t) - f(x_1(t), z_1(t)) - g(z_2(t))u(t) + v(t) + \lambda \dot{e}_1(t) + k_i e_1(t). \quad (23)$$

By setting $\dot{s}(t) = 0$, the equivalent control law can be obtained as

$$u_{eq}(t) = g^{-1}(z_2(t))(\ddot{y}_{1d}(t) + \lambda \dot{e}_1(t) + k_i e_1(t) - f(x_1(t), z_1(t))). \quad (24)$$

where $\lambda$ and $k_i$ are selected such that the polynomial $\ddot{e}_1(t) + \lambda \dot{e}_1(t) + k_i e_1(t)$ becomes Hurwitz. Applying the control law (24) into (23) yields the resulting error dynamics

$$\dot{s}(t) = \ddot{e}_1(t) + \lambda \dot{e}_1(t) + k_i e_1(t) = v(t), \quad |v(t)| < \overline{v} \quad (25)$$

where $\overline{v}$ is the upper bound of the bias term. If the bias term $v(t)$ is zero, then we obtain the ideal error dynamics

$$\dot{s}(t) = \ddot{e}_1(t) + \lambda \dot{e}_1(t) + k_i e_1(t) = 0, \quad (26)$$

However, the bias term $v(t)$ prevents the tracking error $e_1(t)$ from converging to zero. To suppress this bias term, we choose to use the switching control input as [18]:

$$u_{sw}(t) = g^{-1}(z_2(t)) k_{sw} sgn(s(t)). \quad (27)$$

where $k_{sw}$ is a positive constant, $k_{sw} \geq \overline{v} + \eta$ where $\eta$ is a positive constant, and the signum fuction $sgn(\cdot)$ is defined as

$$sgn(x) = \begin{cases} -1, & \text{if } x < 0 \\ 0, & \text{if } x = 0 \\ 1, & \text{if } x > 0. \end{cases} \quad (28)$$

Combining the equivalent and switching control laws, we have the complete control law as:

$$u(t) = u_{eq}(t) + u_{sw}(t) = g^{-1}(z_2(t))(\ddot{y}_{1d}(t) + \lambda \dot{e}_1(t) + k_i e_1(t) - f(x_1(t), z_1(t))) + g^{-1}(z_2(t)) k_{sw} sgn(s(t)). \quad (29)$$

This control scheme (Fig. 2) consists of three elements. The feedback term $g(z_2(t))^{-1}(-\lambda \dot{e}_1(t) - k_i e_1(t))$ makes the closed-loop system stable within a uniform error bound; the term $-g(z_2(t))^{-1}(f(x_1(t), z_1(t)))$ cancels system nonlinearity; the switching input $-g(z_2(t))^{-1} k_{sw} sgn(s(t))$ suppresses the bias term $v(t)$.

### *C. Stability analysis*

To prove stability of the closed-loop system, we select a Lyapunov function candidate as:

$$V(t) = \frac{1}{2} s^2(t). \quad (30)$$

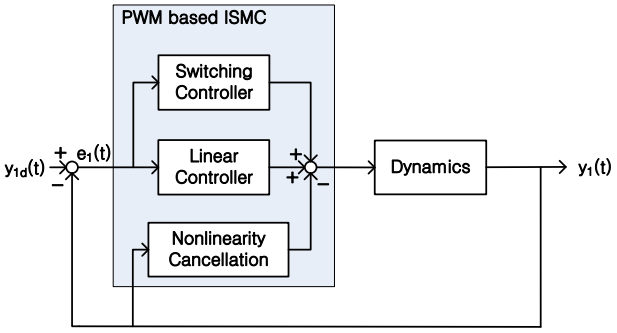


Fig. 2. The schematic diagram of control system for the Cuk converter.

Taking the derivative of the Lyapunov function candidate with respect to time, we have

$$\dot{V}(t) = s(t)\dot{s}(t). \tag{31}$$

Applying the control law (23) into (31) yields

$$\begin{aligned}\dot{V}(t) &= s(t)(\ddot{y}_{1d}(t) - f(x_1(t), z_1(t)) - g(z_2(t))(u_{eq}(t) \\ &\quad + u_{sw}(t)) + v(t) + \lambda\dot{e}_1(t) + k_i e_1(t)) \\ &= s(t)(v(t) - k_{sw} sgn(s(t))) \\ &= -k_{sw}|s(t)| + s(t)v(t) \\ &\leq -k_{sw}|s(t)| + |s(t)|\overline{v} \\ &\leq -|s(t)|(k_{sw} - \overline{v}) \\ &\leq -\eta(|s(t)|) \\ &\leq -\eta\sqrt{V}. \end{aligned} \tag{32}$$

Therefore, the state trajectory reaches the surface $s(t) = 0$ in a finite time $T_f$ and remains there even under the presence of the bias term [22]. Since $s(t) = 0$ for all $t > T_f$, it follows that $\dot{s}(t) = 0$ for all $t > T_f$. For $s(t) = 0$, $e_1(t)$ stays on the following error dynamics

$$\ddot{e}_1(t) + \lambda\dot{e}_1(t) + k_i e_1(t) = 0. \tag{33}$$

Because $\lambda$ and $k_i$ are chosen such that the polynomial $\ddot{e}_1(t) + \lambda\dot{e}_1(t) + k_i e_1(t)$ becomes Hurwitz in (26), $e_1(t)$ converges to zero exponentially fast.

*Remark 1.* Discontinuous switching control usually results in chattering that may excite undesirable high frequencies or unmodeled dynamics. The chattering phenomenon can be suppressed by using smoothing approximation of a sign function. A saturation function can serve as an example that can replace a sign function with [13]:

$$\text{sgn}(s(t)) \rightarrow \text{sat}(s(t)/\phi), \tag{34}$$

where $\phi > 0$ represents the thickness of the boundary layer, which should be adjusted to achieve an optimal balance of tracking performance and chattering reduction. Then, the resulting control law can be written as

$$\begin{aligned}u^*(t) &= g^{-1}(z_2(t))(\ddot{y}_{1d}(t) + \lambda\dot{e}_1(t) + k_i e_1(t) \\ &\quad -f(x_1(t), z_1(t))) + g^{-1}(z_2(t))k_{sw}\text{sat}(s(t)/\phi). \end{aligned} \tag{35}$$

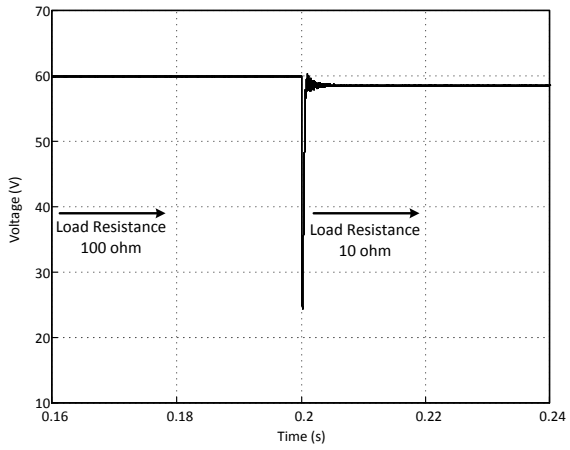


(a)

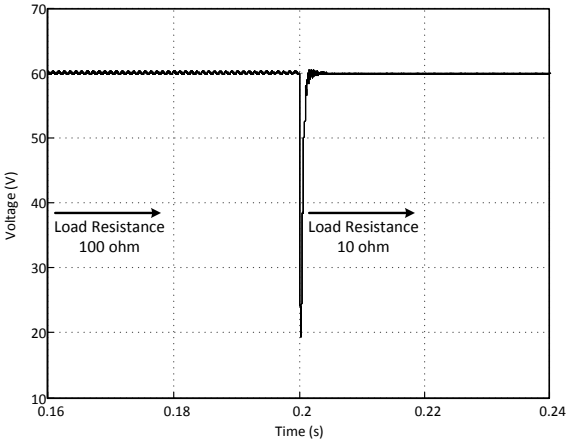


(b)

Fig. 3. Simulation waveforms of output voltage in load change. (a) The equivalent control. (b) Plus the switching control.

## IV. Simulation Results

To show the feasibility of the developed controller, various computer simulations is conducted with a Cuk converter model. The dynamics of the Cuk converter are given as

$$\frac{dx_1(t)}{dt} = x_2(t), \tag{36}$$

$$\begin{aligned}\frac{dx_2(t)}{dt} &= \left(-\frac{1}{L_2C_2} + \frac{1}{(R_LC_2)^2}\right)x_1(t) - \frac{1}{R_LC_2^2}z_1(t) \\ &+\frac{1}{L_2C_2}z_2(t)u(t) + \Delta v(x_1(t), z_1(t), z_2(t), d(t)), \end{aligned} \tag{37}$$

$$y_1(t) = x_1(t), \tag{38}$$

where we set the input voltage $V_i = 50\ V$, the desired output voltage $V_{do} = 60\ V$, the capacitance $C_1 = 1\ \mu F$, $C_2 = 100\ \mu F$, the inductance $L_1 = 500\ uF$, $L_2 = 500\ uF$, and the switching frequency $f_s = 50\ kHz$. The control input is selected as

$$\begin{aligned}u^*(t) &= g^{-1}(z_2(t))(\ddot{y}_{1d} + \lambda\dot{e}_1(t) + k_i e_1(t) \\ &-f(x_1(t), z_1(t))) + g^{-1}(z_2(t))k_{sw}\text{sat}(s(t)/\phi), \end{aligned} \tag{39}$$

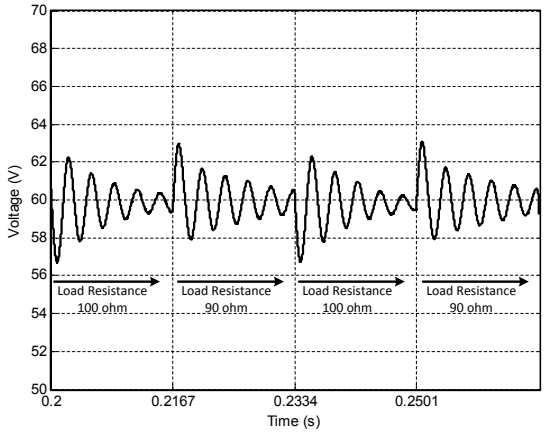


(a)

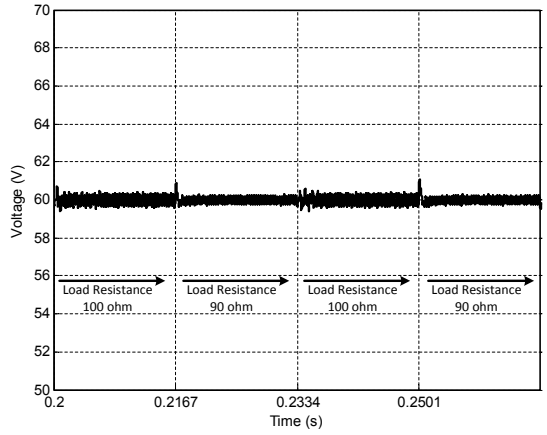


(b)

Fig. 4. Simulation waveforms of output voltage subject to load change from 100 to 90 ohm at 30 Hz. (a) the equivalent controller. (b) plus the switching controller.

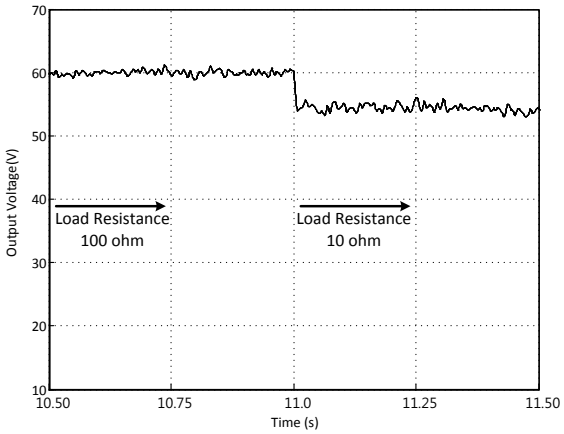


(a)

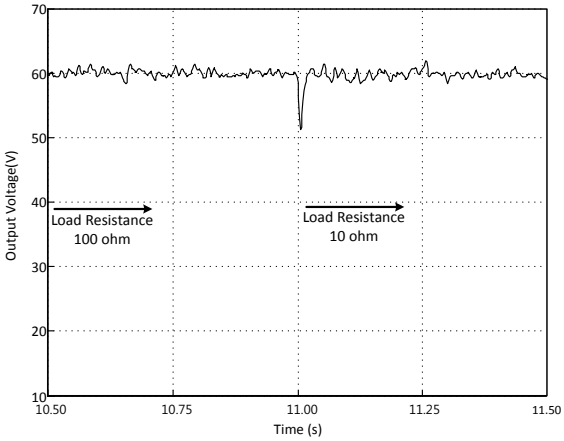


(b)

Fig. 5. Experimental waveforms of output voltage in load change. (a) The equivalent control. (b) Plus the switching control.

where we set $\lambda = 2\times10^7$, $k_i = 4\times10^4$, $k_{sw} = 4.6\times10^4$, $\phi$ = 0.1. We simulate this example with the PSIM software.

Under the above setting and the unit step input command $v_{do} = 60\ V$, we tested the equivalent plus switching controller subject to the load resistance $R_L = 100\ \Omega$ for the first 0.2 seconds and $R_L = 10\ \Omega$ afterward. When the equivalent control input is used, the output voltage changes from 60 V to 25 V as load resistance is changed at 0.2 second. Afterward, the output voltage tracks the step input command with a steady state error ($\simeq$ 1.5 V) (Fig. 3(a)). When the ISMC with the switching controller is used, the transient response is similar but the steady-state error of the closed-loop system is much smaller than that of the system with the equivalent controller (Fig. 3(b)).

To demonstrate the performance of the proposed controller, we examined the rms errors of the unit step input responses in Table I. The rms error of the proposed controller is smaller than that of PD controller plus nonlinear cancellation term.

Figs. 4(a), 4(b) show the simulation performance of the Cuk converter operating at 30-Hz step-load change. Output voltage ripple of the Cuk converter with the PWM-based ISMC is smaller than that with the PD controller plus nonlinear cancellation term. So, the Cuk converter with the PWM-based ISMC tracks the desired voltage better under dynamic load change condition.

## V. Experiment

To demonstrate practical feasibility of the developed controller, the proposed control algorithm was applied to an experimental prototype of the Cuk converter. The controller was developed utilizing the MPC5554EVB reference board, and state variables such as the output voltage and duty ratio were obtained using CANoe software tool.

TABLE I
RMS ERRORS AT STEADY-STATE AFTER LOAD CHANGE

| Controller | Simulation | Experiment |
|---|---|---|
| The equivalent control | 1.5369 V | 5.3369 V |
| Plus the switching control | 0.2753 V | 0.6391 V |

We set the unit step input command ($v_{do} = 60\ V$) and control parameters as $\lambda = 1.3\times10^7$, $k_i = 9\times10^4$, and

TABLE II
PARAMETERS AND COMPONENTS OF THE PROTOTYPE CUK CONVERTER

| Parameters | Symbols | Value |
|---|---|---|
| Input voltage | $v_i(t)$ | 50 V |
| Desired output voltage | $v_{do}$ | 60 V |
| Switching frequency | $f_s$ | 50 kHz |
| First capacitance | $C_1$ | 2.5 $\mu$F |
| Second capacitance | $C_2$ | 280 $\mu$F |
| First inductance | $L_1$ | 1 mF |
| Second inductance | $L_2$ | 1 mF |
| **Components** | **Symbols** | **Part number** |
| Switch | $S_1$ | IXTX200N10L2 |
| Gate Driver | $G_1$ | SKHI 22B R |
| Diode | $D_1$ | E20U60DN |

$k_{sw} = 1.8 \times 10^4$. The main components and parameters of the prototype used for experiments were shown in Table II.

We tested the converter equipped with the PD controller plus nonlinear cancellation term and the ISMC. The performance of the PD controller plus nonlinear cancellation term was poor subject to load variation (Fig. 5(a)). The output voltage is about 60 V before the load resistance changes, but it dropped below 55 $V$ after the load resistance changes. When the ISMC was used, the switching control input suppressed the disturbance produced by the load variation, thereby eliminating the steady-state error (Fig. 5(b)).

To demonstrate the performance of the proposed controller, we examined the rms errors of the unit step input responses in Table I. As we use the proposed controller, the rms error becomes significantly smaller than that of PD plus nonlinear cancellation.

## VI. CONCLUSION

This paper presented a fixed-frequency PWM based ISMC for the Cuk converter. The fourth-order model of the Cuk converter is derived first and then simplified. Based on the simplified model, the ISMC is developed and applied to the Cuk converter. The exponential stability of the closed-loop system is derived. We compare the performances of the PD controller plus nonlinear cancellation term and the ISMC by using the simulation and experimental results and verify that the proposed controller is superior in tracking accuracy.

## REFERENCES


[1] B. K. Kushwaga and A. Narain, "Controller Design for Cuk Converter Using Model Order Reduction", *in International Conference on Power, Control and Embedded Systems (ICPCES)*, 2012, PP. 1-5.

[2] G. Su, W. Gong, L. Pan, R. Gao, and B.B. Wang, "Maximum power point tracking of photovoltaic", *in Chines Control Conference (CCC)*, Jul. 2010, pp. 4880-4884.

[3] H.S.H.Chung, K.K.Tse, S.Y.R.Hui, C.M.Mok, and M.T.Ho, "A novel maximum power point tracking technique for solar panels using a SEPIC or Cuk converter", *IEEE Transactions on Power Electronics*, vol. 18, no. 3, pp. 717-724, May 2003.

[4] Y.Fan, L.M.Ge, and W.Hua, "Multiple-input DCDC converter for the thermoelectric-photovoltaic energy system in hybrid electric vehicles", *in IEEE Vehicle Power Propulsion Conference*, Aug. 2010, pp. 35-40.

[5] J. Knight, S. Shirsavar and W. Holderbaum, "An Improved Reliability Cuk Based Solar Inverter With Sliding Mode Control", *IEEE Transactions on Power Electronics*, vol. 21, no. 4, pp. 1107-1115, Jul. 2006.

[6] T. H. Kim, N. V. Sang, and W. Choi, "Control of The Portable Fuel cell charger using Cuk converter", *IEEE Transactions on Power Electronics*, vol. 2, no. 5, pp. 1655-1667, May 2013.

[7] V. S. C. Raviraj and P. C. Sen, "Comparative study of proportional-integral, sliding mode, and fuzzy logic controllers for power converters", *IEEE Transactions on Industry Applications*, vol. 33 no. 2, pp. 518-524, Mar./Apr. 1997.

[8] S. P. Huang,H. Q. Xu, and Y. F. Liu, "Sliding-mode controlled Cuk switching regulator with fast response and first-order dynamic chacteristic", *in Annual IEEE Power Electronics Specialists Conference*, Jun. 1989, pp. 124-129.

[9] L. Malesani, L. Rossetto, G. Spiazzi, and P.Tenti, "Performance Optimization of Cuk Converters by Sliding Mode Control", *IEEE Transactions on Power Electronics*, vol. 10, no. 3, pp. 302-309, May 1995.

[10] Z. Chen, "PI and Sliding Mode Control of a Cuk Converter", *IEEE Transactions on Power Electronics*, vol. 27, no. 8, pp. 3695-3703, Aug. 2012.

[11] S. Tan, Y. M. Lai, and C. K. Tse, "General Design Issues of Sliding-Mode Controllers in DC-DC Converters", *IEEE Transactions on Industry Electronics*, vol. 55, no. 3, pp. 1160-1174, Mar. 2008.

[12] V. M. Nguyen and C. Q. Lee, "Indirect implementations of sliding-mode control law in buck-type converters", *in IEEE Applied Power Electronics Conference*, Vol. 1, Mar. 1996, pp. 111-115.

[13] V. Utkin and J. Shi, "Integral Sliding Mode Control in Systems Operating under Uncertainty Conditions", *in IEEE Conference On Decision and Control (CDC)*, Dec. 1996, pp. 4591-4596.

[14] R. K. Lea, R. Allen and S. L. Merry, "A comparative study of control techniques for an underwater flight vehicle", *in International Journal of Systems Science*, vol. 30, no. 9, pp. 947-964, 1999.

[15] M. Fu, X. Bian, W. Wang and J. Gu, "Research on sliding mode controller with an integral applied to the motion of underwater vehicle", *in IEEE International Conference on Mechatronics and Automation*, 29 Jul.-1 Aug. 2005, vol. 4, pp. 2144-2149.

[16] Z. Tang, J. Zhou, X. Bian and H. Jia, "Simulation of optimal integral sliding mode controller for the depth control of AUV", *in IEEE International Conference*

*on Information and Automation (ICIA)*, Jun. 2010, pp. 2379-2383.

[17] J. Shi, H. Liu and N. Bajcinca, "Robust control of robotic manipulators based on integral sliding mode", *in International Journal of Control*, vol. 81, no. 10,, pp. 1537-1548, Oct. 2008.

[18] J. J. Slotine, and W. Li, *Applied nonlinear control*, New Jersey: Prentice hall 1991.

[19] P. Mattavelli, L. Rossetto, G. Spiazzi, and P. Tenti, "General-purpose sliding-mode controller for DC/DC converter applications", *in IEEE Annual Power Electronics Specialists Conference*, Jun. 1993, pp. 609-615.

[20] S. C. Tan, Y. M. Lai, M. K. H. Cheung, and C. K. Tse, "On the practical design of a sliding mode voltage controlled buck converter", *IEEE Transactions on Power Electronics*, vol. 20, no. 2, pp. 425-437, Mar. 2005.

[21] S. C. Tan, Y. M. Lai, C. K. Tse, and C. K. Wu, "A Pulsewidth Modulation Based Integral Sliding Mode Current Controller for Boost Converters", *in IEEE Annual Power Electronics Specialists Conference*, Jun. 2006, pp. 1-7.

[22] H. K. Khalil, *Nonlinear systems*, vol. 3, Upper Saddle River: Prentice HALL 2002.

[23] S. C. Tan, Y. M. Lai, C. K. Tse, and M. K. H. Cheung, "A Fixed-Frequency Pulsewidth Modulation Based Quasi-Sliding-Mode Controller for Buck Converters", *IEEE Transactions on Power Electronics*, vol. 20, no. 6, pp. 1379-1392, Nov. 2005.